Case Report

Spontaneous membranoproliferative glomerulonephritis in a young Crl:CD-1(ICR) mouse

Tomoaki Tochitani[1*], Mami Kouchi[1], Yuta Fuji[1], Yuka Yoshino[1], and Izumi Matsumoto[1]

[1] Preclinical Research Unit, Sumitomo Dainippon Pharma Co., Ltd., 3-1-98 Kasugade-naka, Konohana-ku, Osaka 554-0022, Japan

Abstract: Here, we reported a spontaneous case of membranoproliferative glomerulonephritis observed in a young ICR mouse. A 5-week-old female mouse was euthanized owing to abdominal swelling and increased body weight. At necropsy, generalized subcutaneous edema, and clear, colorless, non-viscous ascites were observed. Histologically, the kidneys showed diffuse, bilateral glomerular lesions. The lesions were characterized by thickening and double contour of the basement membrane and an increase in mesangial cells and matrix, resulting in the narrowing of the capillary lumen. Additionally, eosinophilic hyaloid material accumulated in the subendothelial areas and Bowman's space. The material was positive for periodic acid-Schiff, complement component C3, or immunoglobulin G, stained red by Masson's trichrome, and stained blue by phosphotungstic acid-hematoxylin stain and was considered to be plasma due to glomerular leakage. The glomerular lesion was diagnosed as membranoproliferative glomerulonephritis, and an uncertain endothelial injury was suspected as the cause. (DOI: 10.1293/tox.2019-0081; J Toxicol Pathol 2020; 33: 177–181)

Key words: spontaneous lesion, membranoproliferative glomerulonephritis, Crl:CD-1(ICR) mouse

Here, we report a spontaneous case of membranoproliferative glomerulonephritis (MPGN) observed in a young Crl:CD-1 (ICR) mouse, a strain frequently used in toxicity studies.

A 5-week-old female ICR mouse was received from the Charles River Laboratories Japan, Inc. (Kanagawa, Japan) and placed in quarantine. Two days after receipt, the animal presented with abdominal swelling and a marked increase in body weight (from 21.9 g at receipt to 28.0 g). Therefore, 3 days after the receipt, the animal was euthanized by exsanguination from the axillary artery and vein under isoflurane anesthesia and necropsied. The procedures for animal care and housing were in compliance with the institutional guidelines for the care and use of laboratory animals.

Blood biochemical tests were performed using serum sampled at necropsy. For histopathological examination, the kidneys, adrenal glands, heart, liver, lung, skeletal muscle, and spleen were fixed in 10% neutral buffered formalin, paraffin-embedded, sectioned, and stained with hematoxylin and eosin (HE). Additionally, kidneys sections were stained with periodic acid-Schiff (PAS), periodic acid-methenamine-silver (PAM), Masson's trichrome (MTC), phosphotungstic acid-hematoxylin (PTAH), and direct fast scarlet (DFS) methods. For immunohistochemistry, kidneys sections were subjected to a labeled polymer method using the Histofine MOUSESTAIN KIT or Simple Stain Mouse MAX-PO (Nichirei Biosciences Inc., Tokyo, Japan) for antibodies against CD31 (product No.: ab28364; prediluted; Abcam, Cambridge, UK), smooth muscle actin (SMA; clone: 1A4; product No.: M0851; prediluted; Dako, Glostrup, Denmark) and C3 (clone: EPR19394; product No.: ab200999; 1:1000; Abcam), or directly against endogenous mouse immunoglobulin G (IgG), and were counterstained with hematoxylin. The validity of the positive staining was assessed using negative control slides, in which the primary antibodies were substituted with antibody diluents. For electron microscopic examination, small pieces of the kidney fixed in neutral buffered 10% formalin were refixed in 2.5% glutaraldehyde, postfixed in 1% osmium tetroxide, and routinely embedded in Epon resin. Ultrathin sections of the selected areas were prepared, contrasted with hafnium chloride and lead citrate, and examined using an HT7700 transmission electron microscope (Hitachi High-Technologies Corp., Tokyo, Japan).

At necropsy, generalized subcutaneous edema, and clear, colorless, non-viscous ascites were observed. Blood biochemical tests revealed low levels of total protein, albumin, and calcium, as well as high levels of blood urea nitrogen, total cholesterol, triglycerides, phospholipids, phosphorus, and potassium (Table 1).

Histologically, bilateral and diffuse glomerular lesions were observed. The capillary walls were thickened, and the mesangial area was expanded, resulting in narrowing of the capillary lumen (Fig. 1A). Along the capillary walls or with-

---

in the Bowman's space, eosinophilic hyaloid material was accumulated. Furthermore, in some Bowman's capsules, swelling or basophilia of parietal epithelial cells and thick-ening of the basal membrane were observed. The thickened capillary walls, expanded mesangial areas, and accumulated material along the capillary walls and in the Bowman's

Table 1. Blood Biochemistry

Parameters	Unit	Present case	Normal mice[a]	
			Mean	SD
Total protein	g/dL	2.5	4.8	0.1
Albumin	g/dL	0.8	1.6	0
Albumin/Globulin		0.47	0.5	0.02
Blood urea nitrogen	mg/dL	161	19	6
Creatinine	mg/dL	0.2	0.1	0
Glucose	mg/dL	201	234	18
Total cholesterol	mg/dL	232	84	7
Triglyceride	mg/dL	272	81	31
Phospholipid	mg/dL	344	159	18
Phosphorus	mg/dL	16.8	4.9	0.2
Calcium	mg/dL	3.2	9.4	0.2
Sodium	mEq/L	152	150	2
Potassium	mEq/L	7.1	4.2	0.2
Chloride	mEq/L	113	115	2

[a]The results for normal mice are obtained from 8-week-old female Crl:CD-1 (ICR) mice (N=3) of the same lot as the present case that was assigned to a toxicity study and were dosed with vehicle (0.5% methylcellulose water solution) by oral gavage once daily for 2 weeks. SD, standard deviation.
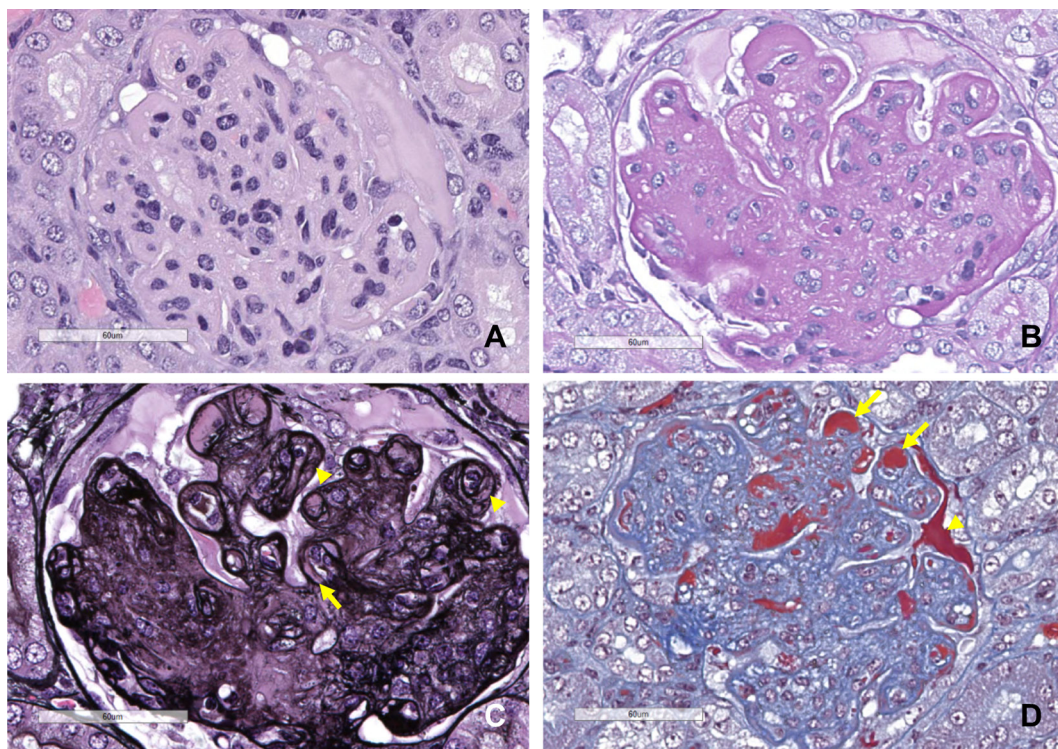

Fig. 1. HE- and special-stain images of the glomeruli. (A) Capillary walls thicken and the mesangial area is expanded resulting in narrowing of the capillary lumen. Within the Bowman's space, eosinophilic hyaloid material is accumulated (arrow). Also, in the Bowman's capsule, swelling or basophilia of parietal epithelial cells can be observed. HE. (B) The thickened capillary tufts and expanded mesangial areas are positive for periodic acid-Schiff (PAS). (C) The collapse of tufts, thickening and double contour of the basement membrane (arrowheads) and increase of mesangial cells and matrix can be seen. The hyaloid material is negative for periodic acid-methenamine-silver (PAM) and observed in subendothelial areas (arrow). PAM. (D) The hyaloid material in subendothelial areas (arrows) and Bowman's space (arrowhead) is stained red by Masson's trichrome (MTC).

space were all positive for PAS (Fig. 1B). The PAM stain revealed collapsed tufts, thickening and double contour of the basement membrane, and an increase in mesangial cells and matrix (Fig. 1C). The hyaloid material was negative for PAM and was observed in subendothelial areas. Red blood cells were sometimes observed in the mesangial areas or between the double-contoured basement membrane. The hyaloid material was stained red by MTC (Fig. 1D), stained blue by PTAH, and was negative for DFS.

Immunohistochemistry for CD31 confirmed the narrowing of the capillary lumen (Fig. 2A). Furthermore, increased expression of SMA was observed in the mesangial and subendothelial areas, suggesting activation, proliferation, and interposition of mesangial cells (Fig. 2B). The hyaloid material was generally positive for IgG (Fig. 2C) and C3 (Fig. 2D); it was negative for IgG in the subendothelial areas.

Electron microscopically, amorphous, electron-dense deposits were observed in the subendothelial areas (Fig. 3A and B).

In the kidneys, other than in the glomeruli, tubular basophilia mainly in the cortex, as well as minimal tubular vacuolation and hyaline cast were observed. No remarkable changes were observed in the blood vessels and interstitium. Other than in the kidneys, only minimal arteritis in the heart, and minimal to mild extramedullary hematopoiesis in the adrenal glands and spleen were observed.

The glomerular lesion was diagnosed as MPGN based on histological characteristics such as basement membrane thickening and mesangial cell proliferation, according to INHAND[1]. Accumulation of hyaloid material is also a characteristic of hyaline glomerulopathy; however, unlike in the present case, in hyaline glomerulopathy, mesangial proliferation is usually not observed, and hyaloid material is ultrastructurally observed as microtubular or fibrillary structures[2].

MPGN is a light microscopic pattern of injury that can be caused by several diseases, and detailed morphological characteristics such as the presence and location of immune complex deposits are important to investigate the cause of MPGN[3]. In the present case, the accumulation of hyaloid material was characteristically observed in the glomeruli. The special stains and immunohistochemical evaluations suggested that this material included plasma proteins such as fibrin, IgG, and C3. Additionally, this material was observed in the subendothelial areas and Bowman's space, while it was not obvious in the basement membrane or subepithelial areas. Therefore, the material was deemed as plasma due to glomerular leakage, rather than immune complex deposits. Reportedly, similar lesions, called insudative lesions, can be
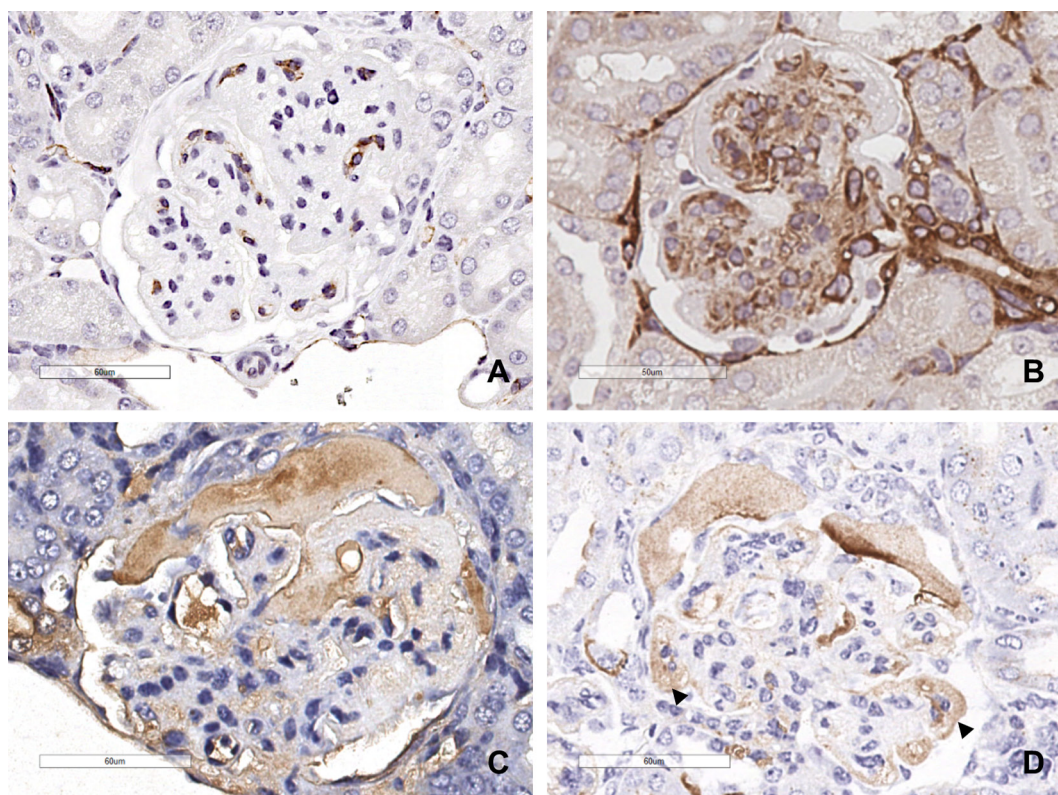

Fig. 2. Immunohistochemistry for CD31 (A), smooth muscle actin (SMA; B), IgG (C), and C3 (D). Capillary lumen is narrowed, while SMA expression is increased in the mesangial and subendothelial areas. The material accumulated in the Bowman's space, as well as plasma in the capillary lumen, is positive for IgG, while the capillary walls are negative. On the other hand, the material in both the Bowman's space and subendothelial areas (arrowheads) is positive for C3.
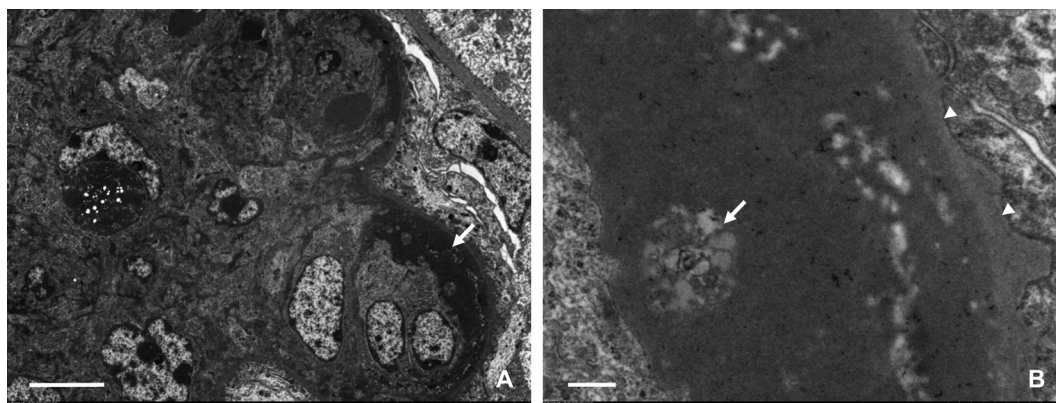
Fig. 3. Electron microscopy of the glomeruli. (A) Electron dense material can be observed along the capillary wall (arrow). Bar=50 μm. (B) Higher magnification of (A). The electron dense material can be observed in the subendothelial area. Relatively electron-lucent, irregularly-shaped material can also be seen (arrow). The basement membrane is indicated by the arrowheads. Bar=5 μm.

observed in glomerular diseases such as diabetic nephropathy and thrombotic microangiopathy[4, 5], and an association with endothelial injuries has been suggested[6]. Furthermore, chronic endothelial injury can demonstrate the MPGN pattern without immune complex deposits[3, 7]. Thus, in the present case, an uncertain endothelial injury was suspected as the cause of MPGN. It has been reported that the loss of vascular endothelial growth factor (VEGF) in podocytes leads to endothelial injury and thrombotic angiopathy in mice[8]. However, in the present case, changes in VEGF expression could not be demonstrated using immunohistochemistry (data not shown), and the possible mechanism of endothelial injury was unknown. Moreover, the relationship between glomerular lesions and minimal arteritis in the heart remained uncertain.

In mice, spontaneous MPGN has been reported in mice deficient in factor H (FH), the principal inhibitor of the alternative pathway of the complement system[9]. However, the glomerular lesion in FH-deficient mice is distinct from the present case and is characterized by global deposition of C3 along the capillary wall; and insudative lesions have not been reported in FH-deficient mice. Additionally, a mutant strain ICR-derived glomerulonephritis (ICGN) mouse spontaneously develops nonproliferative glomerular lesions accompanied by hypoproteinemia and hypercholesterolemia as early as 40 days of age[10]. The glomerular lesion in ICGN can be distinguished from the present case by the absence of mesangial cell proliferation even in the terminal stage and presence of spike-like protrusions in the basement membrane, with deposition of immunoglobulin along the capillary wall. Furthermore, spontaneous glomerular lesions have been reported in a 33-day-old female and an 8-week-old male ICR mice[11, 12], and the morphological characteristics are similar to those in the present case, including capillary wall thickening, the double contour of the basement membrane, and subendothelial accumulation of hyaloid material or plasma component negative for Congo red. Although some differences have been observed such as in

the presence of hypoproteinemia, mesangial proliferation, or stainability of accumulated material for immunoglobulins and C3, this could be reflective the difference in the disease stages.

Here, we presented a spontaneous case of MPGN observed in a young ICR mouse. Though further research is needed to clarify the incidence and pathogenesis of spontaneous MPGN in young ICR mice, we believe that this report could provide relevant information for pathological examinations in toxicity studies.

Disclosure of Potential Conflicts of Interest: Authors declared no potential conflicts of interest with respect to the research, authorship, and/or publication of this article.

Acknowledgements: We wish to thank Ms. Izuru Mise for her excellent histotechnical work.

References

1. Frazier KS, Seely JC, Hard GC, Betton G, Burnett R, Nakatsuji S, Nishikawa A, Durchfeld-Meyer B, and Bube A. Proliferative and nonproliferative lesions of the rat and mouse urinary system. Toxicol Pathol. 40(4 Supple): 14S–86S. 2012. [Medline] [CrossRef]
2. Kouchi M, Toyosawa K, Matsumoto I, Michimae Y, Tochitani T, Koujitani T, Okimoto K, Funabashi H, and Seki T. Hyaline glomerulopathy with tubulo-fibrillary deposits in young ddY mice. Toxicol Pathol. 39: 975–979. 2011. [Medline] [CrossRef]
3. Masani N, Jhaveri KD, and Fishbane S. Update on membranoproliferative GN. Clin J Am Soc Nephrol. 9: 600–608. 2014. [Medline] [CrossRef]
4. Raparia K, Usman I, and Kanwar YS. Renal morphologic lesions reminiscent of diabetic nephropathy. Arch Pathol Lab Med. 137: 351–359. 2013. [Medline] [CrossRef]
5. Matsui K, Sato H, Yokoyama Y, Egawa M, and Ito T. Nephrotic syndrome caused by thrombotic microangiopathy during bevacizumab treatment for lung metastases after

rectal cancer surgery: A case report. Shimane J Med Sci. 35: 21–25. 2018.

6. Mise K, Yamaguchi Y, Hoshino J, Ueno T, Sekine A, Sumida K, Yamanouchi M, Hayami N, Suwabe T, Hiramatsu R, Hasegawa E, Sawa N, Fujii T, Hara S, Sugiyama H, Makino H, Wada J, Ohashi K, Takaichi K, and Ubara Y. Paratubular basement membrane insudative lesions predict renal prognosis in patients with type 2 diabetes and biopsy-proven diabetic nephropathy. PLoS One. 12: e0183190. 2017. [Medline] [CrossRef]

7. Fogo AB, and Kashgarian M. Diagnostic Atlas of Renal Pathology, 3rd ed. Elsevier, Amsterdam. 2017.

8. Eremina V, Jefferson JA, Kowalewska J, Hochster H, Haas M, Weisstuch J, Richardson C, Kopp JB, Kabir MG, Backx PH, Gerber HP, Ferrara N, Barisoni L, Alpers CE, and Quaggin SE. VEGF inhibition and renal thrombotic microangiopathy. N Engl J Med. 358: 1129–1136. 2008. [Medline] [CrossRef]

9. Pickering MC, Cook HT, Warren J, Bygrave AE, Moss J, Walport MJ, and Botto M. Uncontrolled C3 activation causes membranoproliferative glomerulonephritis in mice deficient in complement factor H. Nat Genet. 31: 424–428. 2002. [Medline] [CrossRef]

10. Ogura A, Asano T, Matsuda J, Takano K, Nakagawa M, and Fukui M. Characteristics of mutant mice (ICGN) with spontaneous renal lesions: a new model for human nephrotic syndrome. Lab Anim. 23: 169–174. 1989. [Medline] [CrossRef]

11. Shibuya K, Tajima M, Yamate J, and Kudow S. Idiopathic glomerulopathy in a young ICR mouse. J Comp Pathol. 103: 107–111. 1990. [Medline] [CrossRef]

12. Ago K, Sugahara G, Shirota K, and Kurata Y. Spontaneous early-onset glomerulonephritis in a 8-week-old male Crj:CD1 (ICR) mouse. J Toxicol Pathol. 28: 237–241. 2015. [Medline] [CrossRef]